

# The Band-Sampled-Data collection for the search of continuous gravitational wave signals

1<sup>st</sup> Ornella Juliana Piccinni

*INFN, Sezione di Roma*

*Physics department, Universita di Roma Sapienza*

Rome, Italy

ornella.juliana.piccinni@roma1.infn.it

2<sup>nd</sup> Sergio Frasca

*INFN, Sezione di Roma*

*Physics department, Universita di Roma Sapienza*

Rome, Italy

sergio.frasca@roma1.infn.it

**Abstract**—The detection of gravitational wave signals in the LIGO and Virgo interferometric detector data, is possible thanks to the application and development of several data analysis techniques and to the improvement in the detector sensitivity. A particular type of signal, still undetected by the LIGO-Virgo collaboration, is the so-called continuous wave signal (CW). A CW signal is a quasi-monochromatic signal, deeply buried in the data and modulated by several physical effects. In order to extract the signal from the detector noisy data, several data handling and manipulations should be performed. In particular this type of gravitational wave is recovered using techniques from Fourier analysis and phase demodulations. In this work we will present a new data framework called Band-Sampled-Data (BSD) collection developed for all the searches of CW signals, and the main features of the data used in this context will be described.

**Index Terms**—Continuous waves, LIGO-Virgo, reduced-analytic signal

## I. INTRODUCTION

Gravitational waves (GW) are ripples in the space-time generated by astrophysical sources such as black holes and neutron stars. In order to measure those tiny deformation of the space-time, an advanced generation of Earth-based interferometric antennas (LIGO and Virgo) have been developed during the last years [1], [2]. Nine months of data were taken in the last observational run (O2), running from November 2016 to August 2017. The LIGO and Virgo detectors, which are based on a modified version of a Michelson interferometer, measure space-time deformations induced by passing gravitational waves, by monitoring the relative variation of the light optical path in the two arms. The displacements that need to be measured are of the order of  $10^{-18}$  m. Each interferometer produces a calibrated time-series, known as  $h(t)$ . The  $h(t)$  stream, which contains the reconstructed GW strain channel, is sampled at 16384 Hz. The data of the detector present different noise sources which should be monitored during the runs. Several data analysis techniques have been developed in order to extract the signal from the noise.

The first direct detection of GW happened in September 2015 during the first observational run (O1), almost 100 years later than the theoretical prediction by Einstein, and was followed by other five detections. All the signals detected so far have been produced by the coalescence of two massive bodies, a pair of black holes or a pair of neutron stars.

Among the possible GW signals detectable by LIGO and Virgo antennas, there are those produced by fast spinning neutron stars both isolated or in binary systems. This type of signal is called continuous wave (CW), due to its long-lived nature. This work is organized as follows: in Sec. II the CW signals will be reviewed, in Sec. III a new data analysis framework for the search of CW signals will be described. In Sec. IV a technique used to correct this signal from several physical effects will be shown. Sec. V shows some applications of the framework while Sec. VI is left for conclusions.

## II. CONTINUOUS GRAVITATIONAL WAVE SIGNAL

The main sources for CW signals are fast spinning asymmetric neutron stars (NSs). These are expected to emit a long-lived signal and with a well defined waveform: a nearly sinusoid with frequency slightly varying over times much longer than the observational time.

### A. The signal model

A CW signal emitted by a rotating non-axisymmetric neutron star, steadily spinning around one of its principal axis, is described at the detector site as [3]:

$$h(t) = \text{Re} \left( H_0 \left( H_+ A^+(t) + H_\times A^\times(t) \right) e^{j(\omega(t)t + \Phi_0)} \right) \quad (1)$$

where  $\omega(t)$  is the time dependent angular frequency, while  $\Phi_0$  is an initial phase. The emitted signal frequency  $f_0$  at a given time  $t_0$ , is related to the star rotational frequency by  $f_0 = \frac{\omega(t_0)}{2\pi} = 2f_{rot}(t_0)$ . The complex amplitudes  $H_+$  and  $H_\times$  are given, respectively, by:

$$H_+ = \frac{\cos 2\psi - j\eta \sin 2\psi}{\sqrt{1 + \eta^2}} \quad (2)$$

$$H_\times = \frac{\sin 2\psi + j\eta \cos 2\psi}{\sqrt{1 + \eta^2}} \quad (3)$$

where  $\psi$  is the polarization angle. This is defined as the counter-clockwise angle between the polarization ellipse semi-major axis and the source celestial parallel. The parameter  $\eta$ , which is given by the ratio of the polarization ellipse semi-minor to semi-major axis, indicates the degree of polarization of the GW, and takes values in the range  $[-1, 1]$  ( $\eta = 0$  for

a linearly polarized wave,  $\eta = \pm 1$  for a circularly polarized wave).

The time dependent functions  $A^+$ ,  $A^\times$ , are the detector response to a passing GW and depend on the source position, the detector location and its orientation on the Earth. They produce a splitting of the signal power among the five angular frequencies  $\omega_0$ ,  $\omega_0 \pm \Omega_\oplus$  and  $\omega_0 \pm 2\Omega_\oplus$ , where  $\Omega_\oplus$  is the Earth sidereal angular frequency.

Due to the Doppler effect, the signal frequency at the detector  $f(t)$  is related to the emitted frequency  $f_0(t)$  by<sup>1</sup>

$$f(t) = \frac{1}{2\pi} \frac{d\Phi(t)}{dt} = f_0(t) \left( 1 + \frac{\vec{v} \cdot \hat{n}}{c} \right) \quad (4)$$

where  $\vec{v} = \vec{v}_{orb} + \vec{v}_{rot}$  is the detector velocity in the Solar System Barycenter (SSB), sum of the Earth's orbital and rotational velocity, while  $\hat{n}$  is the versor pointing to the source position. The emitted signal frequency slowly decreases with time due to the rotational energy loss of the star, consequent to the emission of electromagnetic radiation and gravitational radiation. This spin-down can be described by a Taylor series expansion:

$$f_0(t) = f_0 + \dot{f}_0(t - t_0) + \frac{\ddot{f}_0}{2}(t - t_0)^2 + \dots \quad (5)$$

where  $[\dot{f}_0, \ddot{f}_0, \dots]$  are the so called spin-down parameters. There are also other smaller relativistic effects, namely the Einstein delay and the Shapiro delay, which may play a role for long coherence times.

### B. CW searches

Accordingly to the information available about the source, several type of searches can be set up. The computational cost of a given search increases when there is less information about the source. The parameter space we need to investigate is a  $(4 + N)$ -dimensional space, which consist in the source sky position, and the intrinsic source rotational parameters (frequency, spin-down, and higher  $N+1$  order of the frequency derivatives). The main CW searches can be divided in:

- *blind all-sky searches*: for neutron stars (isolated or in binary systems) with no electromagnetic counterpart. No information about the source is used.
- *Directed searches*: for NSs at specific known locations with unknown frequency and spin-down (e.g. searches pointing to the Galactic Center or to supernova remnants). The source position is assumed as known or a small portion around the source sky position is investigated.
- *Narrow-band and targeted*: in the case of signals emitted by known pulsars, i.e. with rotational parameters and sky position well known (targeted) or known with a small uncertainty (narrow-band).

The data analysis techniques of the previously mentioned searches would be characterized by the search sensitivity, its robustness towards instrumental noise and uncertainties and by its total computational cost.

<sup>1</sup>This relation is valid in the non-relativistic approximation  $v/c \ll 1$ .

For instance, coherent methods, based on matched filtering, can be used to gain signal-to-noise ratio in targeted searches, which are characterized by a good sensitivity and a low computational cost. On the other hand, when less or no information about the source is available, like in the case of all-sky searches, hierarchical methods have been developed in order to explore a large volume of the source parameter space. The number of parameters that can be investigated in this type of searches is limited by the computational power available. In between those two extreme cases in terms of sensitivity and computational cost are placed the narrow-band and the directed searches.

A recent review of the latest observational results and methods can be found in [4] and [5].

### III. THE BAND-SAMPLED-DATA COLLECTION

As mentioned in II-B, there exists several types of CW searches. Each of them is characterized by a different setup and a different sensitivity. In particular the sensitivity of a given search is related to the coherence time. In targeted and narrow-band searches, the coherence time is equal to the total observational time; while in incoherent or hierarchical searches (directed or all-sky), the data stream is divided in chunks, analyzed coherently and then incoherently combined. The duration of the coherence time is chosen using different criteria and from this chunk of data FFTs are built. The new data framework, called "Band-Sampled-Data" collection (BSD), consists in a set of band-limited time series, down-sampled and divided in sub-bands, partially cleaned from instrumental disturbances. Each time series is contained in a file (called BSD file) covering a frequency band of 10 Hz and spanning one month of data. Two contiguous frequency bands are non-overlapped since we expect that several instrumental lines lie at frequencies proportional to 10 Hz. With this choice the event rate of detections is not affected in any substantial way. The data contained in the BSD files are in the form of what we call *reduced-analytic signals* (see III-B), where the time series is complex-valued rather than real-valued, with no negative frequency component [6], [7]. One of the differences between the classical analytic signal and its corresponding reduced-analytic form is that the sampling frequency is equal to the bandwidth. In order to allow a simple handling and processing of the data for the different types of analysis, several MATLAB routines have been developed. Starting from the standard settings of BSD files, which is a band of 10 Hz and 1 month of data, it is possible, for instance, to extract a sub-band which covers more than 1 month of data or join more frequency bands for a shorter time span, see Fig. 1. Making a comparison with the old architecture (see [8]), the BSD collection can be seen as a database made up by a multitude of sub-databases (the BSD files) each with a suggested FFT duration per each 10 Hz frequency band. For semi-coherent searches the time duration of the data chunks to be incoherently combined (the FFT length), can be chosen in a optimal way for each frequency band, rather than being fixed. Barycentric and spin-down corrections are applied by means

of a “sub-heterodyne” technique, consisting in multiplying the data by a phase shift function, as described in Sec. IV.

The entire procedure of BSD production is computationally cheap and fast. As an example, the total disk usage for the production of a full set of BSD files, covering 4 months of data, 1024 Hertz and 2 antennas, is about 260 GB, while the total creation time is of few hours on a standard workstation CPU. Within this new framework the data handling is very simple and easily allows to use the data also for searches of other gravitational wave signals (different from CW), like transients. In fact, different file *configurations* can be chosen, depending on the specific analysis to be done. For instance, for all-sky or directed searches, which are based on a semi-coherent approach, a suitable configuration could consist of a set of files covering a band of 10 Hz and 1 month of data. For targeted or narrow-band searches, on the other hand, for which a full-coherent analysis is done over a very small frequency band, a better choice would be building the BSD files over, e.g., 1 Hz and covering the full observation time of the data. In the case of searches for long transients signals, characterized by a very large frequency variation in time, a reasonable choice could be building files which cover hundreds of Hertz in frequency and a few hours, or even minutes, in time.

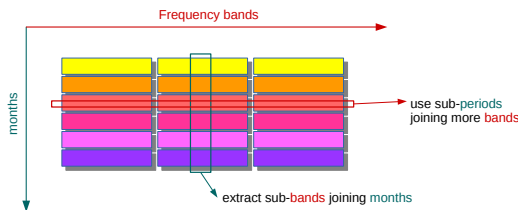


Fig. 1. The Band Sample Data collection can be seen as a database of sub-databases. Data handling functions allow to efficiently extract subsets of the data or to combine data both in time and frequency.

### A. BSD creation

We will focus now on the practical construction of the BSD database. Starting from the collection of FFTs (called SFDB) described in [8], the range of frequencies between 10 Hz and 1024 Hz is split in bands of width  $\Delta f_{BSD}=10$  Hz. For each band of each FFT the following steps are applied, see Fig. 2:

- compute the inverse Fourier transform and subsample to the inverse of the band width (i.e with a sampling time of  $\frac{1}{\Delta f_{BSD}}$  seconds);
- create the *reduced-analytic signal* (see Sec. III-B);
- remove the first and the last quarter of the time domain series, in order to avoid redundancies due to the overlapping in time (by half) of the FFTs<sup>2</sup>.
- store this piece of data stream into the BSD file.

These operations are repeated for all the FFTs contained in the SFDB file and the whole process is iterated for all the

<sup>2</sup>In the SFDBs the FFTs are produced by chunks of data interlaced by half in time. Selecting the central part of the new time series, we ensure that the data will not contain any artifact produced by the truncation of the original data stream into chunks

frequency bands until the entire detector band is covered. More details about the BSD preparation are given in Secs. III-B and III-C. In order to reduce the Input/Output bottleneck when the

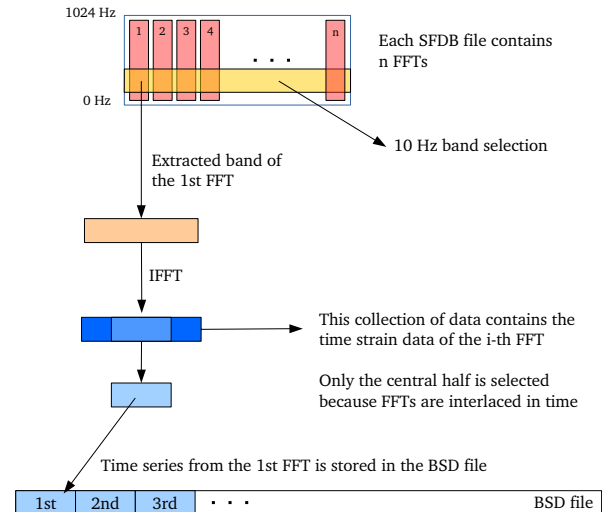


Fig. 2. BSD preparation scheme. BSD files are created from the SFDB files which contain a number  $n$  of FFTs (pink blocks). For each frequency band of, e.g.,  $\Delta f_{BSD} = 10$  Hz (yellow block) extracted from a FFT (orange), data are inverse Fourier transformed (blue + light blue block), and the central half is selected (light blue) and stored in the BSD file.

FFTs in the SFDB are accessed for reading, the procedure works on several bands simultaneously (generally up to 10), depending on the available computer memory.

Processed data are stored in a versatile format, called *gd*, implemented in the MATLAB-based software *Snag*<sup>3</sup>. A BSD file contains the data stored in the *gd* format, plus extra informations about the data, stored in an auxiliary structure. This data auxiliary structure contains, among other information, the starting time of the BSD (in MJD - Modified Julian Date), defined as the time of the first sample of the *gd*; the initial frequency of the band; the band width covered by the file; the velocity and the position (in units of  $c$ ) of the detector in the Solar-System-Barycenter frame and the reference time of those values; the detector data structure; the run name; the calibration version of the used data; the cleaning information and other minor ones.

### B. The analytic signal and its reduced form

In this section we discuss in more detail the type of data stored in the time series of the BSD. The data stored in a BSD file derive from the analytic signal, is a complex-valued time series without negative frequency components. From the Hermitian symmetry of the Fourier transform, in the analytic representation of a signal the negative frequency components of the Fourier transform can be discarded, with no loss of information.

From the point of view of signal reconstruction, in a standard analytic signal the sampling frequency is equal to that of the original real valued signal, i.e. at least two times the

<sup>3</sup>Snag website: <http://www.roma1.infn.it/~frasca/snag/default.htm>

maximum frequency of the band, as required by the Nyquist theorem. In fact, our data are sampled exactly at the maximum frequency of the band, after shifting the initial frequency to 0 Hz, e.g. at 10 Hz, if the data cover a band of 10 Hz, see Fig. 3. Such signal is called (in this context) *reduced-analytic*, because the sampling frequency is half the one used for analytic signals. However there exists a perfect equivalence between the analytic signal and the reduced-analytic signal: indeed the reduced-analytic signal can be obtained taking only the odd time samples of an analytic signal. By using appropriate normalization factors a reduced-analytic signal with the following properties can be built: a) the amplitude (in time) of the complex reduced-analytic signal is half that of the starting real data; b) the power spectrum of the reduced-analytic signal is the same as that of the starting real data. A specific MATLAB function, which converts the reduced-analytic signal in its real version using the correct sampling frequency, has been developed to check this equivalence. Since we mostly analyze data in the frequency domain (e.g. using Fourier transforms) rather than in time domain, we decided to set the power spectrum equal to that of the original data.

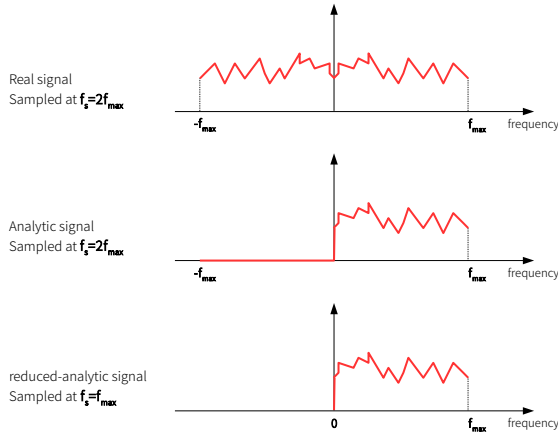


Fig. 3. Top plot: the Fourier transform of a real valued function would appear with both positive and negative frequency components, which are symmetric around zero due to the Hermitian symmetry. The sampling frequency in this case must be (as required by the Nyquist theorem) at least twice the maximum frequency  $f_s = 2f_{max}$ , in order to avoid aliasing. Middle plot: in the analytic representation of a real-valued function, the negative frequency components are set to zero, while the sampling frequency is the same as in the real-valued case. Bottom plot: our data are built discarding the negative-zero component of a classical analytic signal and it is sampled exactly at the maximum frequency of the positive band (the sampling is then half the sampling frequency used for the analytic signal). A perfect equivalence exists between the analytic and the reduced-analytic signal.

### C. Data cleaning

BSD data are cleaned using various techniques. First, the short FFTs database used to build the BSD are vetoed for non-science segments (i.e. data corresponding to time periods when the detector was not locked or not working properly are set to zero) and subject to a cleaning step where big, short duration time disturbances are removed [8]. A further cleaning step is applied to the BSD data, which again consists in zeroing large time-domain disturbances which appear after band extraction

(and not visible in the starting time series as their power is confined in a small frequency band). This is done by excluding samples above a given threshold. The threshold is taken, after a study based on real detector data, as  $\theta_{thr} = 10 \times m_l$  where  $m_l$  is an estimate based on the median of the average detector noise.

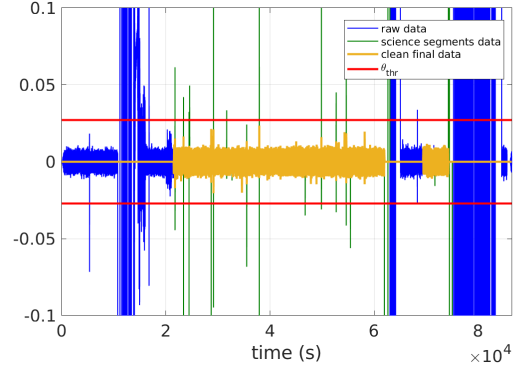


Fig. 4. Time strain data (in units of  $10^{-20}$ ) before any cleaning is shown in blue. The selection of science data is done directly during SFDB construction (green). On the BSD time series a further cleaning step is performed to remove residual large time-domain disturbances higher than a given threshold  $\theta_{thr}$  (yellow: final cleaned data).

As an example, for O1 data the fraction of data excluded with this choice is around 2% for LIGO Livingston detector and 1% for LIGO Hanford, see Fig. 4. This is by purpose a *conservative* cleaning. An extra cleaning procedure which deletes the more persistent lines and apply a time-frequency filter, built adaptively to the data, can be also applied, see Sec.XIII in [9], and [10].

## IV. THE SUB-HETERODYNE CORRECTION

A CW signal is modulated mainly by the Doppler shift and by the intrinsic spin-down of the source, as described in Sec.II. Such effects must be properly taken into account in order to increase signal detectability. One standard technique, used to correct the signal, is a data re-sampling. This method consists in a re-definition of the time variable, see e.g. [11] and this change of variable is independent of the signal frequency. However, re-sampling can be too computationally expensive. Indeed, the number of samples needed to re-define the time variable (with enough precision) for signals with high frequency, is very large. An alternative way to correct a signal is to use an ad hoc heterodyne phase correction which is particularly suitable for the BSD architecture. Let us assume that the frequency and spin-down parameters  $[f_0, \dot{f}_0, \ddot{f}_0, \dots]$  for a given source are known at the reference time  $t_0$ . The signal phase shift due to the source spin-down can be written as (from Eq. 5)

$$\phi_{sd}(t) = 2\pi \int_{t_0}^t \left[ \dot{f}_0(t' - t_0) + \frac{1}{2} \ddot{f}_0(t' - t_0)^2 + \dots \right] dt'. \quad (6)$$

From Eq. 4 the Doppler frequency shift is given by

$$\Delta f_{Dopp} = f_0(t) \left( \frac{\vec{v} \cdot \hat{n}}{c} \right). \quad (7)$$

The corresponding phase factor is, apart from an irrelevant constant term:

$$\phi_d(t) = 2\pi \int_{t_0}^t f_0(t') \frac{\vec{v} \cdot \hat{n}}{c} dt' \approx \frac{2\pi}{c} p(t) f_0(t), \quad (8)$$

where  $p(t)$  is the position of the detector in the SSB projected along the source sky position  $\hat{n}$ . The function  $p(t)$  is obtained interpolating the samples of the detector position which are stored in the auxiliary data structure. The final phase factor, containing both the Doppler and the spin-down terms is simply the sum of the two phases:

$$\Phi_{corr}(t) = \phi_d(t) + \phi_{sd}(t). \quad (9)$$

The effect of the Doppler shift and spin-down can then be corrected by multiplying the BSD data by the exponential factor  $e^{-j\Phi_{corr}(t)}$ :

$$y(t) = [h(t) + n(t)] e^{-j\Phi_{corr}(t)} \quad (10)$$

where  $h(t)$  is the strain amplitude of a GW signal in the detector, while  $n(t)$  is the detector noise. In this way a hypothetical signal becomes monochromatic except for some residual modulations  $\delta\Phi = \omega(t)t + \Phi_0 - \Phi_{corr}(t)$  which haven't been taken into account (e.g. second order spin-down, or due to slightly wrong position parameters of the source). After the correction there is still an amplitude modulation due to the non-uniform antenna pattern, which spreads the signal power at five frequencies, which can be used to build a detection statistic and to estimate signal parameters [3], [11].

## V. POSSIBLE APPLICATIONS OF THE BSD FRAMEWORK

Among the possible applications of the BSD framework, the most intuitive one is for targeted searches. Since we know source frequency and spin-down, we can extract a narrow frequency band, around the expected  $f_0$ , from the BSD database and build a single BSD file spanning the entire run. On this BSD one can apply the heterodyne correction and matched-filtering, similarly to what is currently done [3], but without the need to combine together short (O(1000) s long) data chunks and working at a much reduced sampling rate (10 Hz against 4096 Hz). Timing of the code shows that, once the BSD files have been produced, the analysis of one year of data from three detectors for a single target (that is for fixed values of the sky position and rotational parameters) takes about 90 core-minutes, which is more than two orders of magnitude better than the old procedure [3]. This means that the analysis of O(200) pulsars, like that described in [12], could be done on the data of the LIGO-Virgo O3 run, planned to start in fall 2018 and to last about one year, in O(300) core-hours. This estimation neglects the time for any follow-up analysis or to compute upper limits.

The same procedure can be used in the follow-up stage of any CW search. Indeed this is a big improvement in the follow-up of candidates of all-sky searches like the one described in [9]. In particular, as in the follow-up stage we are interested in analyzing data in a small region of the parameter space around the candidate, we can use the data around that

particular candidate extracting a BSD sub-band and perform on this small volume a new incoherent search, using a longer coherence time, which implies higher significance and a more accurate parameter estimation. A typical two stages follow-up, with a coherence time increase of a factor of 10, takes about twenty minutes working in the BSD framework, while with the re-sampling method only the signal correction takes O(10) hours for a single detector. This would allow to perform O(10<sup>5</sup>) follow-ups in a few days on a cluster like the ones used in the LIGO-Virgo collaboration.

Another application of BSDs would be a quick look tool for example to search for persistent lines or combs in the power spectrum, based on the cleaning information in the auxiliary time-frequency structure, like the persistency histogram for the identification of noise lines.

## VI. CONCLUSION

In the next generation of GW detectors, the chances to detect continuous wave signals are very high. In order to reach this goal, in parallel with detector enhancements, complex data analysis procedures have been developed with the purpose of having more flexible and computationally efficient pipelines. In this paper we have presented a novel data analysis framework, called Band Sampled Data collection in which, using several signal processing techniques, data can be efficiently prepared for the analysis and manipulated “on-the-fly”, depending on the specific kind of search we want to make. Several applications of the BSD framework have been devised and will be used in most of the next searches for CW signals.

## REFERENCES

- [1] J. Aasi et al, “Advanced LIGO”, *Class. and Quan. Grav.*, vol. 32, p. 074001, 2015
- [2] F. Acernese et al, “Advanced Virgo: a 2nd generation interferometric gravitational wave detector”, *Class. and Quan. Grav.*, vol. 32, p. 024001, 2015
- [3] P. Astone, S. D’Antonio, S. Frasca and C. Palomba, “A method for detection of known sources of continuous gravitational wave signals in non-stationary data”, *Class. and Quan. Grav.*, vol.27, p. 194016, 2010
- [4] C. Palomba, “The search for continuous gravitational waves with LIGO and Virgo detectors”, *Eur. Phys. Soc. Conf. High Energy Phys.*, vol. 5, 2017
- [5] P. D. Lasky, “Gravitational Waves from Neutron Stars: A Review”, *Publ. Astron. Soc. of Aust.*, vol. 32, p. e034, 2015
- [6] D. Gabor, “Theory of communication.”, *J. Inst. Electr. Eng.*, vol. 93, p. 429-441, 1946
- [7] A. Ville, “Theorie et application de la notion du signal analytique”, *IEEE Trans. Acoust.*, vol. 26, p. 467-469, 1978
- [8] P. Astone, S. Frasca and C. Palomba, “The short FFT database and the peak map for the hierarchical search of periodic sources”, *Class. and Quan. Grav.*, vol. 22, p. S1197S1210, 2015
- [9] P. Astone, A. Colla, S. D’Antonio, S. Frasca, C. Palomba, “Method for all-sky searches of continuous gravitational wave signals using the frequency-Hough transform”, *Phys. Rev. D*, vol. 90, p.042002, 2014
- [10] Acernese F. et al, “Cleaning the Virgo sampled data for the search of periodic sources of gravitational waves”, *Class. and Quan. Grav.*, vol. 26, p. 204002, 2009
- [11] Abadie J. et al, “Beating the Spin-down Limit on Gravitational Wave Emission from the Vela Pulsar,” *The Astroph. J.*, vol. 737, p. 93, 2011
- [12] B. P. Abbott et al, “First Search for Gravitational Waves from Known Pulsars with Advanced LIGO”, *The Astroph. J.*, vol. 839, p. 12, 2017